Catalysis Today 175 (2011) 593–597

Contents lists available at ScienceDirect

Catalysis Today

journal homepage: www.elsevier.com/locate/cattod

Structure and catalytic property of supported rhodium catalysts prepared using arc-plasma

Satoshi Hinokuma[a,b], Madoka Okamoto[b], Eriko Ando[b], Keita Ikeue[b], Masato Machida[b,*]

[a] Research Fellow of the Japan Society for the Promotion of Science, Japan
[b] Department of Applied Chemistry and Biochemistry, Graduate School of Science and Technology, Kumamoto University, 2-39-1Kurokami, Kumamoto 860-8555, Japan

ARTICLE INFO

Article history:
Received 18 October 2010
Received in revised form 12 February 2011
Accepted 1 March 2011
Available online 1 April 2011

Keywords:
Arc-plasma
Supported Rh catalyst
$AlPO_4$
CO oxidation

ABSTRACT

A highly dispersed supported Rh catalyst was successfully prepared by an arc-plasma process for the first time and was characterized by means of TEM, XPS and EXAFS. Repeated generation of pulsed arc-plasma using a Rh rod as a cathode was found to deposit crystallized uniform metallic Rh particles with the size of 2.4 ± 1.1 nm onto the surface of $AlPO_4$ powders. The metal-support interaction via Rh–O–P bonding in the catalyst prepared using arc-plasma was found to be weaker than in the catalyst prepared by conventional wet impregnation. The arc-plasma catalyst preparation achieved a higher CO oxidation activity because of highly dispersed metallic Rh nanoparticles.

1. Introduction

Recently, catalyst preparation using plasmas has attracted a lot of attentions [1–4]. According to Liu et al. [3], the potential merit of using plasmas is as follows; (1) a highly dispersed active species; (2) reduced energy requirements; (3) enhanced catalyst activation, selectivity, and lifetime; (4) shortened preparation time. Various thermal and cold plasmas including plasma jet, DC corona, arc, glow-discharge, radio frequency and microwave have been applied to the generation of ultrafine particles, preparation of supported catalysts and/or modification of catalyst surface. These techniques are also quite promising as an innovative approach that lessens the amount of precious metals like Pt, Pd and Rh in catalysts, the demand of which has rapidly increased especially in the field of environmental protection and energy production.

We reported a novel preparation method of supported Pt and Pd catalysts using pulsed arc-plasma [5], which enables the one-step deposition of highly dispersed metal nanoparticles from bulk metals in contrast to the multi-step preparation of conventional wet impregnation processes. In the present work, we have applied this technique to a Rh catalyst supported on $AlPO_4$ to study the local structure and catalytic activity. As was described in our recent reports [6,7], $AlPO_4$ with the tridymite-type structure becomes a robust support material producing optimum interactions with Rh species, which can reduce the threshold loading, owing to the high dispersion of Rh species anchored onto the surface. The outstanding stability of $Rh/AlPO_4$ was demonstrated by thermal ageing in a stream of air, where conventional Rh loaded on Al_2O_3 totally lost its catalytic activity as a result of solid-state reactions at the Rh_2O_3/Al_2O_3 interface. The application of our arc-plasma process is therefore expected to improve further the catalytic performance to $Rh/AlPO_4$.

2. Experimental

2.1. Catalyst preparation

A tridymite-type $AlPO_4$ was prepared from $Al(NO_3)_3$ (Wako Pure Chemicals Ind. Ltd., 99.9%) and H_3PO_4 (Wako Pure Chemicals Ind. Ltd., 85%) as follows. A solution of 0.05 mol of H_3PO_4 in 50 mL of deionized water was added dropwise to a solution containing 0.05 mol of $Al(NO_3)_3$ in 50 mL of deionized water with vigorous stirring. An aqueous ammonia solution (25%) was then added dropwise until the pH of the supernatant was 4.5. The white gel thus obtained was recovered by centrifugation and washed with deionized water for several times. After dried in air at 100 °C, the solid product was calcined in air at 1400 °C for 5 h to yield $AlPO_4$ with the tridymite-type structure. The BET surface area (S_{BET}) of as calcined product was 11 $m^2\,g^{-1}$.

Rh loaded catalysts were prepared using a pulsed cathodic arc-plasma source (Ulvac Inc., ARL-300) with a Rh cathode (ϕ10 mm, 99.99%, Furuya Metals, Co. Ltd.) under vacuum as shown in Fig. 1 [5]. The arc pulse with a period of 0.2 ms and current amplitude of 2 kA was generated with a frequency of 1 or 2 Hz. The plasma

* Corresponding author. Tel.: +81 96 342 3651; fax: +81 96 342 3651.
E-mail address: machida@kumamoto-u.ac.jp (M. Machida).

0920-5861/$ – see front matter © 2011 Elsevier B.V. All rights reserved.
doi:10.1016/j.cattod.2011.03.008

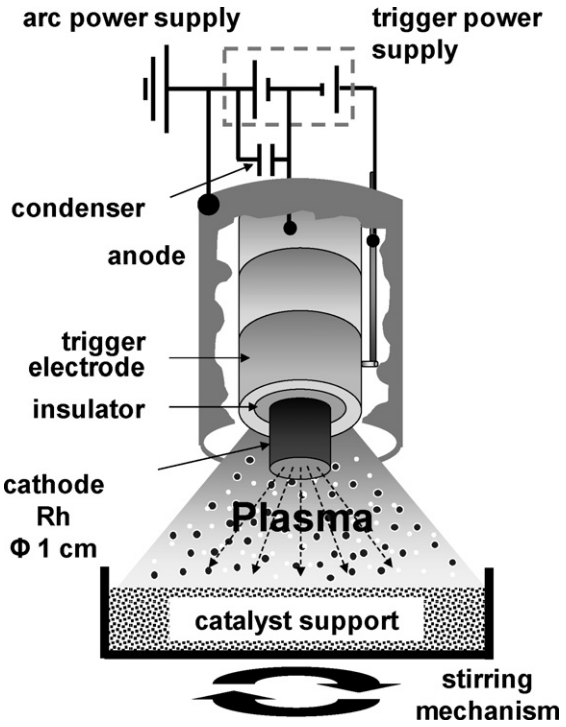

Fig. 1. Schematic illustration of arc-plasma process for preparation of supported Rh catalysts.

from the cathode entered into a container which contains powders of as-prepared $AlPO_4$ under mechanical stirring at ambient temperature. Rh particle size and deposition rate can be controlled by the input energy, which is expressed by $E = (1/2)CV^2$, where C is electric capacity and V is applied discharge voltage. The present study was performed using the following parameters: $C = 360\ \mu F$ and $V = 125$ V. The loading amount of Rh (0.4 wt%) was controlled by the number of pulsing (32,500 shots). The catalysts were also prepared by a conventional wet impregnation method using an aqueous solution of $Rh(NO_3)_3$ (Tanaka Kikinzoku Kogyo Co. Ltd.) and subsequent air-calcination at 600 °C for 3 h. The catalysts prepared by arc-plasma and impregnation methods are denoted as "AP" and "imp", respectively.

2.2. Characterization

X-ray diffraction (XRD) measurement was performed using monochromated Cu Kα radiation (30 kV, 20 mA, Rigaku Multiflex). The content of Rh was determined by X-ray fluorescence measurement (Rigaku EDXL300). High-resolution TEM observation was performed in a FEI TECNAI F20 electron microscope operating at 200 kV. The XPS spectra were measured on a VG Sigmaprobe spectrometer using Mg Kα radiation (15 kV, 20 mA). BET surface area (S_{BET}) was calculated from N_2 adsorption isotherms measured at 77 K (Belsorp-mini, BEL Japan, Inc.).

EXAFS of Rh K-edge was recorded on NW10A station at Photon Factory for Advanced Ring (PF-AR), High Energy Accelerator Research Organization (KEK). A Si(3 1 1) double-crystal monochromator was used. The spectra were recorded at room temperature in a transmission mode. For EXAFS measurement, powder catalysts for XAFS measurement were pressed into a disk of about 1 g to give edge jump of 0.2. The incident and transmitted X-rays were monitored in 17- and 31-cm-long ionization chambers filled with Ar and Kr, respectively. XAFS data were processed using a REX 2000 program (Rigaku). EXAFS oscillation was extracted by fitting a cubic spline function through the post edge region. The k^3-weighted EXAFS oscillation in the 3.0–13.8 Å region was Fourier transformed. For curve-fitting analysis, phase shift and backscattering amplitude functions for Rh–Rh and Rh–O–Rh shells were extracted from the EXAFS data of Rh foil and Rh_2O_3. The curve-fitting analysis for Rh–O–P shell was performed using theoretical parameters.

2.3. Catalytic reaction

Catalytic reaction test for CO oxidation was carried out in a flow microreactor. As-prepared 50 mg of catalyst (10–20 mesh) was fixed in a quartz tube (ϕ6 mm I.D.) by quartz wool at both ends of the catalyst bed. The catalytic activity was evaluated by heating the catalyst bed from room temperature to 600 °C at constant rate of 10 °C min^{-1} with supplying a simulated exhaust gas mixture containing CO (0.1%), O_2 (1.25%) and He (balance) at 100 $cm^3\ min^{-1}$ ($W/F = 5.0 \times 10^{-4}$ g $min\ cm^{-3}$). The effluent gas was analyzed using a Pfeiffer GSD30101 mass spectroscopy and a Horiba VA3000 NDIR CO/CO_2 gas analyzer.

In situ FT-IR spectroscopy was conducted on a Nicolet 6700 spectrometer and a temperature-controllable diffuse reflectance reaction cell with a KBr window that was connected to a gas supply system to allow measurement under controlled gas environments at atmospheric pressure. The sample was first preheated *in situ* in a flowing He at 200 °C for 30 min prior to any experiment. This was followed by cooling to 50 °C, purging with He, and subsequent admission of gas mixtures of 1% CO and He balance for 10 min. Immediately following this procedure, the cell was flushed with a stream of He for 10 min at 50 °C, where spectrum was taken in a stream of He and after subsequent supply of 2.5% O_2/He for 10 min at the same temperature.

3. Results and discussion

3.1. Local structure of Rh catalyst prepared using arc-plasma

Firstly, unsupported Rh particles were prepared by the pulsed arc-plasma technique. Fig. 2(a) shows TEM images of Rh nanoparticles as deposited directly onto a TEM grid covered with microgrid carbon films. Highly dispersed nanoparticles with a uniform size were observed. The histogram analysis clearly suggested a very narrow size distribution ranging from 1 to 5 nm with the average size of 2.3 ± 0.9 nm. The histogram data is also similar to Pt nanoparticles prepared under the same condition in our previous studies [5]. A high resolution structural image in Fig. 2(b) and a FFT pattern (c) proved that these nanoparticles were crystallized metallic Rh with the face-centered cubic structure. Fig. 3 compares TEM images of $Rh/AlPO_4$ as prepared by wet impregnation (imp) and arc-plasma process (AP). Both catalysts showed the presence of Rh nanoparticles deposited on tridymite-type $AlPO_4$ with a grain size of several ten nanometers. The histogram analysis of $Rh/AlPO_4$(AP) exhibited a sharp size distribution with the average size of 2.4 ± 1.1 nm, which was almost the same with the unsupported Rh (Fig. 2). It should be noted that $Rh/AlPO_4$(AP) exhibits a narrower size distribution than $Rh/AlPO_4$(imp) (6.4 ± 5.5 nm), because it is free from the effects of agglomeration and sintering during calcination. Another point to be noted is that the average size and standard deviation were kept unchanged with an increase of Rh loading.

Next we characterized these Rh catalysts by means of XPS and EXAFS. In the Rh 3d XPS spectra (Fig. 4), the peak deconvolution exhibited three $Rh3d_{5/2}$ components of Rh^{3+}, Rh^0, and their intermediate assigned as Rh^+ at the binding energies of 309.5, 306.4 and 308.2 eV, respectively. $Rh/AlPO_4$(AP) contained a considerable amount of Rh^+ species, whereas $Rh/AlPO_4$(imp) was mainly composed of Rh^{3+} species, suggesting that arc-plasma process yielded

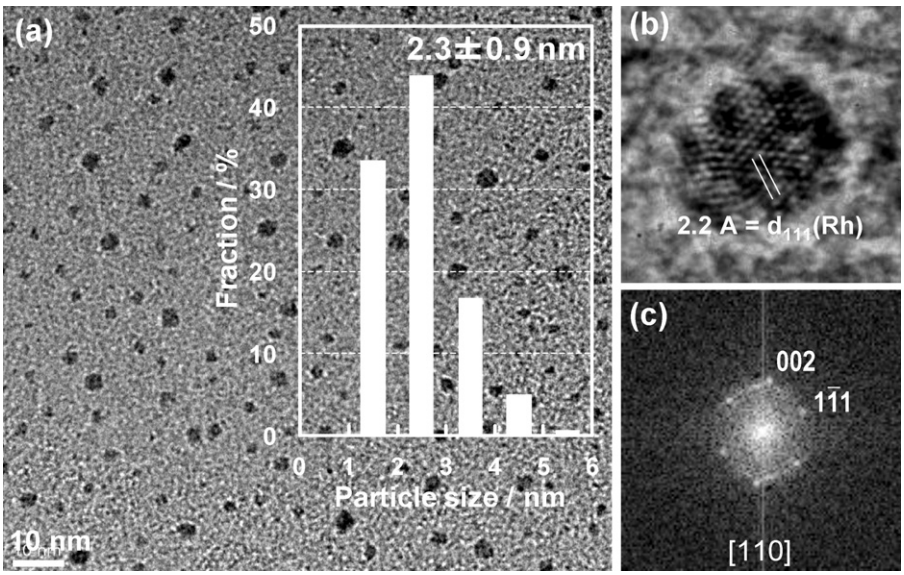

Fig. 2. Unsupported Rh nanoparticles as prepared by arc-plasma process. (a) TEM image and Rh size distribution, (b) high-resolution structure image and (c) FFT pattern.

Rh in lower oxidation states. This is consistent with the results in our previous study on arc-plasma preparation of Pt and Pd catalysts [5]. According to the EXAFS results in the following, the Rh^{+} species in $Rh/AlPO_4$(AP) should be assigned to a metallic Rh, but the shift to a higher binding energy should be attributable to the electron-deficient character of Rh as a result of interaction with $AlPO_4$ support having an acid character.

Fig. 5 shows Fourier transforms of Rh K-edge EXAFS for as-prepared $Rh/AlPO_4$ and two references (Rh and Rh_2O_3) without corrections for phase shifts. The peaks in the Fig. 5 are therefore shifted to shorter *r*-value from true atomic distances. When the first and second coordination shells were filtered, the best curve-fitting was obtained and resultant structural parameters including phase shift corrected *r*-values are shown in Table 1. $Rh/AlPO_4$(imp) catalysts showed the intense peak at around 2.0 Å, which is attributed to a Rh–O shell ($r = 2.03$ Å, $CN = 4.3$), but the second shell was quite different from that of Rh_2O_3. A curve-fitting analysis of the second shell was carefully performed on seven different types of possible shell combinations. The best fitting fit was finally achieved when the contribution of a Rh–O–P shell ($r = 3.09$ Å, $CN = 1.4$) along with Rh–Rh ($r = 2.69$ Å, $CN = 0.32$) was taken into consideration. The formation of Rh–O–P bonding suggests the presence of Rh species strongly interacting with $AlPO_4$ support. On the other hand, $Rh/AlPO_4$(AP) exhibited a much stronger peak due to a Rh–Rh shell ($r = 2.70$ Å, $CN = 2.0$), suggesting the presence of metallic Rh, whereas the coordination number for a Rh–O–P shell was decreased significantly ($CN = 0.55$). From these results, the supported Rh catalyst prepared using arc-plasma can be characterized by (i) the

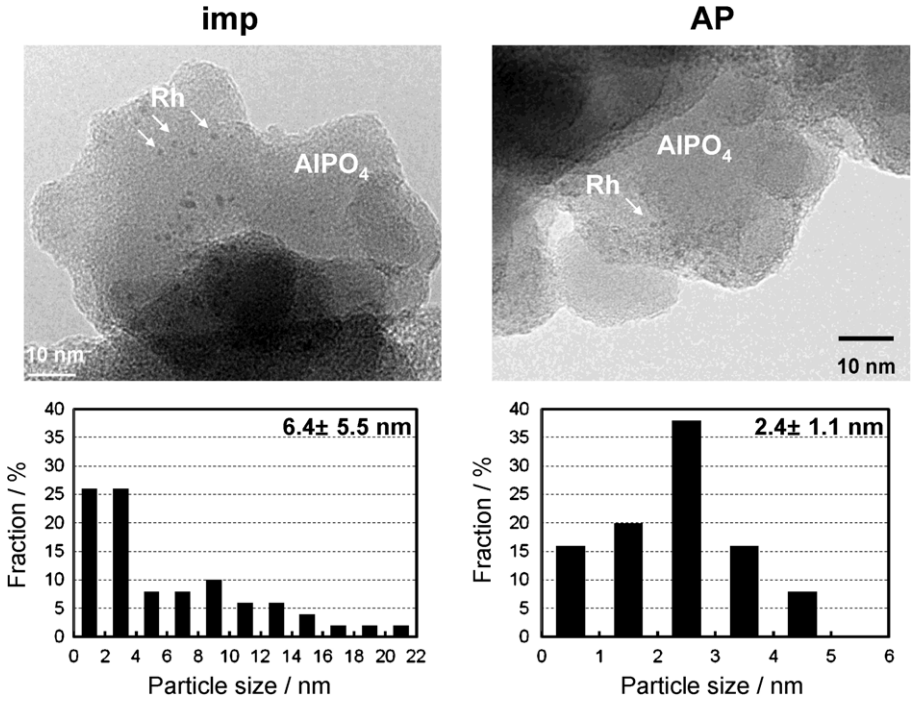

Fig. 3. TEM photographs and Rh size distribution of 0.4 wt% $Rh/AlPO_4$ as prepared by wet impregnation and arc-plasma process.

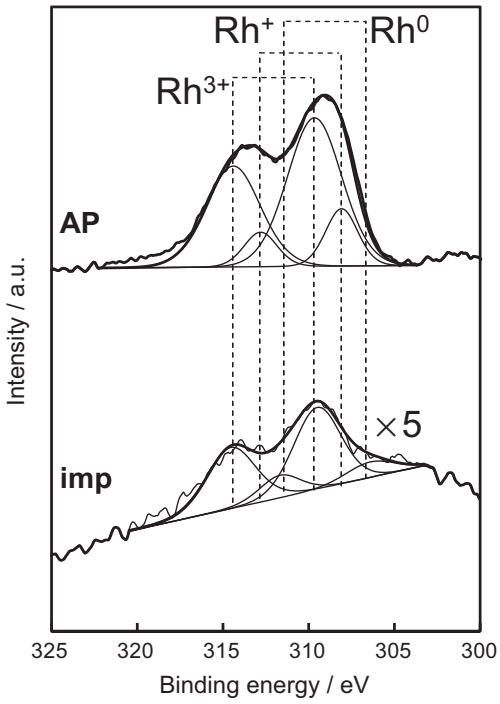

Fig. 4. Rh3d XPS spectra of 0.4 wt% $Rh/AlPO_4$ as prepared by wet impregnation and arc-plasma process.

relative abundance of metallic state and (ii) weaker metal-support interaction. The higher fraction of metallic Rh in $Rh/AlPO_4$(AP) than in $Rh/AlPO_4$(imp) is considered as a common feature of arc-plasma catalyst preparation, which was carried out in vacuum.

3.2. CO oxidation activity of Rh catalyst prepared using arc-plasma

Fig. 6 shows the result of CO oxidation measured in light-off mode using a conventional flow microreactor. As-prepared $Rh/AlPO_4$(AP) initiated the reaction at a low temperature of 100 °C, compared to more than 200 °C required for $Rh/AlPO_4$(imp). The enhancement of catalytic activity by the use of arc-plasma preparation was also observed for C_3H_6 oxidation under oxygen-excess condition. To explain such a catalytic behavior, *in situ* infrared spectra of CO adsorbed on as-prepared $Rh/AlPO_4$ were measured at 50 °C without further reduction pretreatment. Fig. 7 shows the spectra in the range of CO stretching vibration mode. The spec-

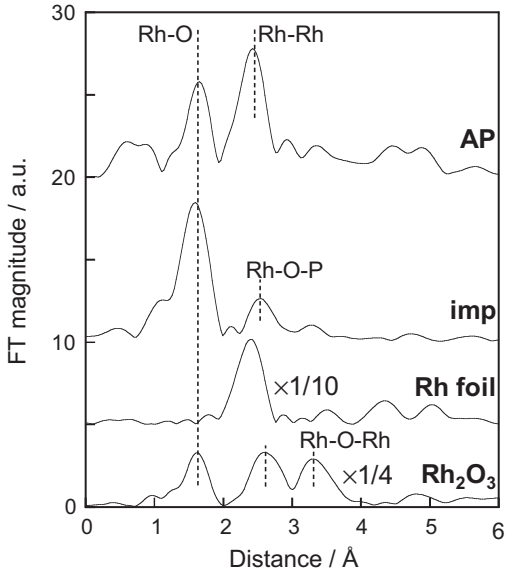

Fig. 5. Fourier transformed Rh K-edge EXAFS for 0.4 wt% $Rh/AlPO_4$ as prepared by wet impregnation and arc-plasma process.

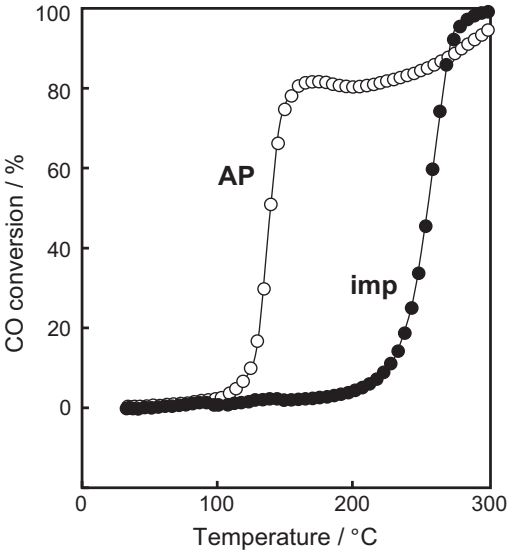

Fig. 6. Light-off of a stream of 0.1% CO and 1.25% O_2 balanced with He for 0.4 wt% $Rh/AlPO_4$ as prepared by (●) wet impregnation and (○) arc-plasma process. Heating rate = 10 °C min^{-1}, $W/F = 5.0 \times 10^{-4}$ g min cm^{-3}.

Table 1
Fitting parameters obtained from Rh K-edge EXAFS analysis of $Rh/AlPO_4$.

	Shell	CN^a (±0.2)	r/Å[b] (±0.03)	$\sigma^2/10^{-2}$ Å^2[c] (±0.05)
$Rh/AlPO_4$(AP)	Rh–O	2.7	2.05	0.15
	Rh–Rh	2.0	2.70	0.42
	Rh–O–P	0.55	3.09	0.36
$Rh/AlPO_4$(imp)	Rh–O	4.3	2.03	0.15
	Rh–Rh	0.32	2.69	0.42
	Rh–O–P	1.4	3.09	0.36
Rh foil	Rh–Rh	12.0	2.69	0.42
Rh_2O_3	Rh–O	6.0	2.04	0.15
	Rh–O–Rh	3.0	2.99	0.23
	Rh–O–Rh	3.0	3.52	0.37
	Rh–O–Rh	6.0	3.75	0.45

Interval of *k*-space to *r*-space of FT is 3.0–13.8 Å^{-1}.
[a] Coordination number.
[b] Atomic distance.
[c] Debye-Waller factor.

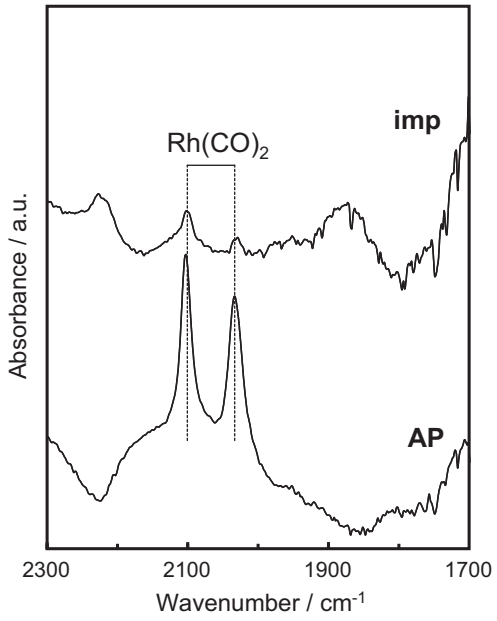

Fig. 7. IR spectra of CO adsorbed on 0.4 wt% $Rh/AlPO_4$ as prepared by wet impregnation and arc-plasma process.

trum for $Rh/AlPO_4$(imp) showed very weak two bands at 2104 and 2035 cm^{-1} assigned to a stretching mode of geminal carbonyl species. On $Rh/AlPO_4$(AP), however, these bands were much stronger than those on $Rh/AlPO_4$(imp), because of their metallic surface suitable for adsorption of CO. When $Rh/AlPO_4$(imp) was pretreated in 10% H_2 at 200 °C for 30 min, CO chemisorption as well as CO oxidation activity were increased to be comparable to those of as-prepared $Rh/AlPO_4$(AP).

Here, it should be noted that the higher frequencies of CO stretching vibration mode (2104 and 2035 cm^{-1}) in Fig. 7, compared to values, 2095 and 2027 cm^{-1}, reported for 2% Rh/Al_2O_3 [8]. The stretching mode of adsorbed CO is known to shift toward higher frequencies with increasing support acidity as a consequence of electronic alteration of supported metals, which is in accordance with the shift of Rh3d XPS signals of metallic Rh as shown in Fig. 4. A similar effect of acidic supports on supported metal catalysts has been reported for various supported metal catalysts [9–14]. The higher shift also implies that the C–O bond is less weakened by chemisorption onto Rh. However, because $Rh/AlPO_4$(AP) and $Rh/AlPO_4$(imp) yielded the bands at the same positions, the shift is not a suitable measure for metal-support interaction of the present system. High dispersion of metallic Rh nanoparticles should play a primary role in catalytic oxidation of CO at low temperatures.

4. Conclusion

$Rh/AlPO_4$ catalyst was prepared by arc-plasma process to study the local structure and catalytic activity for CO oxidation in comparison with the catalyst prepared by conventional wet impregnation. Highly dispersed crystallized metallic Rh particles with the size of 2.4 ± 1.1 nm were deposited on the surface of $AlPO_4$, but metal-support interaction via a Rh–O–P bond was weak. As-prepared catalyst exhibited the higher CO oxidation activity than the impregnated catalyst as a consequence of high dispersion and metallic state of Rh species.

Acknowledgement

This study was supported by Elements Science and Technology Project from MEXT Japan. XAFS experiments were carried out on NW10A of Photon Factory, High Energy Accelerator Research Organization (KEK) (proposal no. 2009G574).

References

[1] M. Boutonnet Kizling, S.G. Järås, Appl. Catal. A: Gen. 147 (1996) 1.
[2] Z.R. Ismagilov, O.Y. Podyacheva, O.P. Solonenko, V.V. Pushkarev, V.I. Kuz'min, V.A. Ushakov, N.A. Rudina, Catal. Today 51 (1999) 411.
[3] C.-j. Liu, G.P. Vissokov, B.W.L. Jang, Catal. Today 72 (2002) 173.
[4] H. Shim, J. Phillips, I.M. Fonseca, S. Carabinerio, Appl. Catal. A: Gen. 237 (2002) 41.
[5] S. Hinokuma, K. Murakami, K. Uemura, M. Matsuda, K. Ikeue, N. Tsukahara, M. Machida, Top. Catal. 52 (2009) 2108.
[6] K. Ikeue, K. Murakami, S. Hinokuma, K. Uemura, D. Zhang, M. Machida, Bull. Chem. Soc. Jpn. 83 (2010) 291.
[7] M. Machida, K. Murakami, S. Hinokuma, K. Uemura, K. Ikeue, M. Matsuda, M. Chai, Y. Nakahara, T. Sato, Chem. Mater. 21 (2009) 1796.
[8] C. Yang, C.W. Garl, J. Phys. Chem. 61 (1957) 1504.
[9] D. Kubička, N. Kumar, T. Venäläinen, H. Karhu, I. Kubičková, H. Österholm, D.Y. Murzin, J. Phys. Chem. B 110 (2006) 4937.
[10] D.C. Koningsberger, D.E. Ramaker, J.T. Miller, J. De Graaf, B.L. Mojet, Top. Catal. 15 (2001) 35.
[11] B.L. Mojet, J.T. Miller, D.E. Ramaker, D.C. Koningsberger, J. Catal. 186 (1999) 373.
[12] M. Primet, J. Catal. 88 (1984) 273.
[13] M. Primet, L.C. De Menorval, J. Fraissard, T. Ito, J. Chem. Soc., Faraday Trans. 81 (1985) 2867.
[14] T.M. Tri, J.P. Candy, P. Gallezot, J. Massardier, M. Primet, J.C. Vedrine, B. Imelik, J. Catal. 79 (1983) 396.